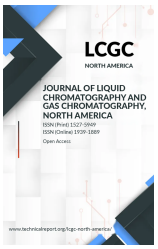

Journal of Liquid Chromatography and Gas Chromatography, North America
https://technicalreport.org/lcgc-north-america/

LC GC N. Am., Vol. 44, No.2, 01-11, 2026

Technical Reports Press

RESEARCH ARTICLE

Validation of Senescence-Specific Proteoforms in the Secretomes of Quiescent and Proliferative Human Fibroblasts

Michael P. Doyle[1*] **and Sayan Pratab**[2]

[1]*Department of Chemistry, The University of Texas at San Antonio, San Antonio, TX 78249, United States*
[*]*Corresponding author*

Corresponding author:
michael.doyle@utsa.edu

Received: 10 September 2025
Accepted: 19 May 2026
Available online: 30 June 2026

Abstract
Proteoform interpretation is necessary for SASP because of secretion as an intact protein, a fully processed variant, as oxidized, cysteinylated, acetylated, phosphorylated, and fragment proteoforms. The goal of the present manuscript is the answer to the question about possibility of generation of defensible validation order using top-down proteomics records of secretomes of senescent, quiescent and proliferating IMR90 fibroblasts, maintaining Context-Anchored Proteoform Scoring (CAPS) calculation. The numerical data include combined secretomes records of senescent, quiescent and proliferating conditions plus seven selective senescent proteoforms: FTL, UBE2V1, HMGA2, DAP, CCL2, TPM3 and EEF1A1. The senescent and proliferating secretomes were very similar in terms of the truncated form pressure, with respective values of 0.67954 and 0.67935, while the quiescent secretome had the lower value of 0.52846. The ratio of senescence-proliferation alignment versus the senescence-quiescence distance was 0.00125, which implies that the abundance of fragment forms is not a criterion for senescence selectivity. The leading senescence selective candidates FTL and UBE2V1 had high leakage-sensitive CAPS values and were relatively easy to confirm. HMGA2 had the highest number of annotated modification sites (4.63 per 100 residues) and needed phosphorylation-specific validation, while DAP and CCL2 needed annotation-resolved confirmation. TPM3 and EEF1A1 remained to be fragment records requiring exploration. To sum up, the answer to the central question is positive – the records can provide a defensible validation order considering control-state form pressure, residue span, modification type, mass agreement, and confirmation burden.

Keywords: cellular senescence, SASP, proteoform, top-down proteomics, intact mass, validation sequence, post-translational modification, secretome

1. Introduction

Cellular senescence is a stress-induced stable cell state during which cells cease proliferation but actively remodel their local environment via secretion and vesicle release. Senescence has been implicated in tumor suppression [1] and wound healing [2], tissue remodelling and development [2] and fibrosis, chronic inflammation, aging, and age-related disorders [3]. Biological effects of senescence are primarily mediated via the senescence-associated secretory phenotype (SASP). It encompasses cytokines, chemokines and growth factors [4], proteases and ECM components [5] and alarmins and vesicular contents [6]. Since SASP promotes tissue healing in one context and causes chronic disease in another, the meaning of any given SASP candidate depends on cell type, control state and molecular form used.

A major challenge in studying SASP is phenotypical heterogeneity. Senescent cells do not express one uniform secretome; their secretions depend on the type of cells, the cause of senescence and the time since induction [7]; the cell metabolic state, chromatin remodeling, DNA damage and mitochondria [8]; and experimental conditions and control type used for discrimination of senescent secretome [9]. A factor distinguishing senescence from quiescence does not distinguish it from proliferation. What appears canonical in one system might be absent, fragmented or altered in another. Recent guidelines on senescence studies emphasize the necessity to report enough information on the

Cite as: M. P. Doyle, S. Pratab. Validation of Senescence-Specific Proteoforms in the Secretomes of Quiescent and Proliferative Human Fibroblasts. LC GC N. Am., 44(2) 2026: 01-11.

experimental context not to interpret individual markers as indicators of senescence. This is particularly important in secretome proteomics due to sample preparation, extracellular processing and state-dependant secretion of SASP molecules.

But the measurement challenge is not only biological but also molecular. A single gene annotation masks terminal processing, proteolysis, oxidation, cysteinylation, phosphorylation, acetylation, alternative sequence variants and modification uncertainty [10]. While this makes the information easy to analyze at the pathway level, it is misleading if a paper claims proteoform-level specificity. A proteoform of a ferritin light chain with three modifications, a proteoform of a UBE2V1 with known chemistry, phosphorylated HMGA2 and truncated TPM3 are different assay problems even if present in the same list of senescence-specific candidates. Therefore, methods for investigation of senescence secretome need to maintain distinction between protein abundance, proteoform identity and validation status [11].

Proteoform-aware proteomics is a direct way of addressing the problem. The proteoform concept acknowledges that a gene product can occur as several molecular species resulting from sequence differences and transcript processing [12] as well as terminal cleavage, proteolysis and post-translational modifications [13]. Further standardization of modified proteoforms and peptidoforms emphasizes the necessity to report the precise molecular form and not just the parent accession or the gene symbol [14]. For the study of senescence biology, this distinction is crucial. Oxidative stress, inflammatory signaling, chromatin remodeling, altered proteostasis and extracellular matrix turnover can change the chemical and structural state of proteins secreted by senescent cells. The molecule form, not just the parent protein, decides what further assay is needed to verify integrity of the mass, phosphopeptides, unknown mass shifts or boundaries of cleavages.

Top-down MS can directly address the problem due to its ability to interrogate intact proteins or proteoforms before enzymatic cleavage thus preserving information about the intact mass and sequence span [15]. It also preserves the information about the combination of modifications [16,17] that can be lost in transition from peptides to protein-level data [18]. Progress in separation technologies, instrumentation, gas-phase fragmentation and proteoform assignment was achieved in the last years [19]. At the same time, the problem of true proteoform characterization is difficult since a table entry can include residue range, theoretical mass, observed mass, modifications, etc. but still not disclose all aspects of the isotope envelope quality, charge-state behaviour, ion support, site localization, replicate dispersion, and chromatographic reproducibility [20]. Therefore, each candidate entry is a lead for validation not a completed claim on biomarker.

The human IMR90 fibroblasts SASP secretome proteomics record provides form classes at condition level and senescence-selective proteoform candidates measured by top-down mass spectrometry [21]. The PRIDE record PXD061829 identifies the same secretome experiment and its Orbitrap Eclipse acquisition context, while PRIDE and ProteomeXchange allow downloading the public proteomics record for the independent review [22]. Condition counts and proteoform features in this record allow posing a specific research question: can dual-condition form pressure and chemistry of proteoforms reveal the set of senescence-selective records ready for immediate validation, those requiring testing for phosphorylation, those needing annotation clarification, and those still remaining fragmentary?

No new computational method is introduced. CAPS is applied as described, and interpretation is based on exact IMR90 condition counts and seven candidate entries. What is questioned here is not whether SASP is rich in truncations but whether this feature allows interpreting truncated forms as senescence-selective when the control cells show nearly the same amount of such forms. Thus, the order of validation becomes different. Entries with defined modification annotations and long spans can remain among the early targets despite a fragment-rich background, while short fragments require more convincing evidence of boundary reproducibility and selective presence in senescent cells. Validation readiness is then treated as weighted proteoform property that depends on residue span, modification identity, mass agreement, presence in control and confirmation burden.

2. Materials and Methods

2.1. Condition Counts and Proteoform Records

The analysis used the IMR90 fibroblast secretome condition counts and the seven specified senescence-selective proteoform records from the top-down mass spectrometry SASP study [21]. Independent verification through PRIDE deposition is consistent with established mass-spectrometry data sharing standards [22]. The analysis uses only the condition counts, residue ranges, masses, modification annotations, and control trace notes reported for the records considered here. Raw spectra, proprietary peak lists, replicate intensities, chromatograms, and additional output were not reprocesed.

The record set consisted of two parts. The condition part included four secretome conditions: combined, senescent, quiescent, and proliferating. For each condition, the preserved counts were signal-peptide-truncated intact class forms, first methionine-truncated intact class forms, intact class forms without any processing, total intact class forms, and total truncated forms. The candidate part included seven proteoforms which have been found in at least three senescent replicates and not in automated outputs of quiescent and proliferating conditions. For each candidate, the preserved data fields were accession, gene symbol, protein description, modification annotation, residue range, theoretical monoisotopic mass, and observed proteoform mass. Low level proliferating traces of each candidate were transformed into sensitivity flags rather than treated as quantitative measurements.

The seven candidates are FTL, UBE2V1, HMGA2, DAP, CCL2, TPM3, and EEF1A1. FTL and UBE2V1 are relatively long proteoform records with defined modification annotations. HMGA2 is a chemically complex, phosphorylation-rich record. DAP and CCL2 are records with annotation uncertainty which complicates interpretation. TPM3 and EEF1A1 are short records with no immediate biomarker value due to their residue range and lack of modification annotations. The seven records therefore require candidate specific validation rules rather than simple abundance comparison.

Table 1: Evidence inventory.

Record group	Specific fields used	Calculated descriptors
Condition form records	Signal-peptide-truncated intact forms, first-methionine-truncated intact forms, unprocessed intact forms, total intact-class forms, total truncated forms	Form pressure, intact-class share, senescence-quiescence distance, senescence-proliferation distance, dual-control alignment ratio
Candidate chemistry records	Gene, accession, residue interval, theoretical mass, observed mass, modification annotation, control-trace flag	Residue span, mass residual, strict CAPS, leakage-sensitive CAPS, modification density, known-modification density, confirmation burden
Validation order records	Candidate identity, conservative score, chemical specificity, control sensitivity	Validation sequence index and assignment to immediate, phosphorylation-specific, annotation-resolved, or exploratory follow-up

As shown by the evidence inventory in Table 1, the validation ordering depends on the contribution of each record type. Condition-form counts determine whether there is an intact-rich or fragment-rich environment that applies to the seven candidate proteoforms. Candidate chemistry decides whether there is enough residue span, mass compatibility, and modification specificity in FTL, UBE2V1, HMGA2, DAP, CCL2, TPM3, or EEF1A1 to warrant any further analysis. Validation-order records ensure that a gene name does not stand for good evidence when the identity of the proteoform is still ambiguous.

2.2. Condition-Level form Pressure

The intact-class count I_c for each condition c was computed as follows:

$$I_c = S_c + M_c + N_c, \tag{1}$$

where S_c denotes signal-peptide-truncated intact forms, M_c denotes first-methionine-truncated intact forms, and N_c denotes unprocessed intact-class forms. The total observed form count was calculated as

$$O_c = I_c + T_c, \tag{2}$$

where T_c is the total truncated-form count. The truncated-form pressure was then defined as

$$F_c = \frac{T_c}{O_c}, \tag{3}$$

and the complementary intact-class share was

$$G_c = 1 - F_c = \frac{I_c}{O_c}. \tag{4}$$

The form pressure value is a contextual metric as opposed to a mechanistic metric. It does not specify a protease, demonstrate intracellular or extracellular cleavage, or separate true biological process from detection artifact. Rather, its task is to describe whether the list of candidates is coming from an environment that is either fragment-rich or intact-rich. This point becomes crucial when interpreting secretomes since there may be processes taking place outside the cells leading to the presence of processed products.

2.3. Proteoform Scoring Anchored by Context

The residue span L_i for each candidate proteoform i was determined from the residue interval:

$$L_i = r_{i,\text{last}} - r_{i,\text{first}} + 1. \tag{5}$$

The absolute monoisotopic mass residual was calculated as

$$E_i = \left| M_{i,\text{obs}} - M_{i,\text{theo}} \right|. \tag{6}$$

The total number of modifications, P_i^*, was determined based on the annotation string. The known number of modifications, K_i^*, consisted of N-terminal acetylation, cysteinylation, oxidation, and phosphorylation. The unknown modifications were considered modification events but not known events, since it is necessary to differentiate between specified modifications and unknown mass shifts in proteoform [20]. The known modification fraction is defined as

$$K_i = \begin{cases} K_i^*/P_i^*, & P_i^* > 0, \\ 0.5, & P_i^* = 0. \end{cases} \tag{7}$$

A neutral value of 0.5 for unmodified records prevents absence of a PTM annotation from being interpreted as either full confidence or complete uncertainty.
The bounded CAPS components were calculated as

$$B_i = \min\left(\frac{L_i}{100}, 1\right), \tag{8}$$

$$C_i = \frac{L_i}{L_{\max}}, \tag{9}$$

$$P_i = \min\left(\frac{P_i^*}{5}, 1\right), \tag{10}$$

$$A_i = 1 - \min\left(\frac{E_i}{1.5}, 1\right), \tag{11}$$

where $L_{\max}$ is the largest residue span among the seven candidates. The strict CAPS value was

$$\text{CAPS}_i^{(0)} = 100\left(0.25B_i + 0.20C_i + 0.25P_i + 0.15K_i + 0.15A_i\right). \tag{12}$$

The leakage-sensitive CAPS value was

$$\text{CAPS}_i^{(L)} = \eta_i \text{CAPS}_i^{(0)}, \tag{13}$$

where $\eta_i = 1$ for candidates that lack low-level control traces and $\eta_i = 0.80$ for candidates that possess low-abundance proliferating traces.
The CAPS score is not a replacement for experimental confirmation. It is a deterministic ranking score that is based on listed table fields. Candidates that possess adequate sequence span, relative coverage, modification annotations, clear identification of modifications, and superior mass agreement will have higher CAPS scores. The leakage-sensitive parameter will impose an additional conservative penalty when a candidate is possibly not entirely excluded from proliferating control samples. The need for conservative treatment is especially critical in view of the differences in behavior of top-down secretome records in terms of peak detection and deconvolution [23] and low-abundance feature identification [20].

2.4. Dual-Control Form-Alignment Analysis

In condition-level analysis, senescence was contrasted with both quiescent and proliferating controls. Two distances were computed:

$$D_{S,Q} = \left| F_S - F_Q \right|, \tag{14}$$

$$D_{S,P} = \left| F_S - F_P \right|. \tag{15}$$

The senescence-proliferation alignment ratio was defined as

$$R_{S,P} = \frac{D_{S,P}}{D_{S,Q}}. \tag{16}$$

The complementary separation share was

$$\Theta_S = \frac{D_{S,Q}}{D_{S,Q} + D_{S,P}}. \tag{17}$$

A small value of $R_{S,P}$ implies that senescence and proliferation are highly correlated along the truncated-form axis despite the difference between senescence and quiescence. A high value of Θ_S means that most of the condition separation was achieved through senescence-quiescence distance rather than separation from proliferation. Such calculations have been done deliberately, since there were no other ways to work with the input, which were merely counts in the tables. Their main advantage is in the prevention of misinterpreting fragment abundance as senescence.

2.5. Modification Density per Residue

Although CAPS features the modification burden feature, the same number of modifications in a short and in a long proteoform means something completely different. Hence, the following values were calculated:

$$\text{MD}_i = 100\frac{P_i^*}{L_i}, \tag{18}$$

$$\text{KMD}_i = 100\frac{K_i^*}{L_i}. \tag{19}$$

The above descriptors represent annotations of events per 100 residues. They do not represent an attempt at defining stoichiometry, site localization probability, or function implication. These are descriptors of candidates where chemical annotation is denser than the size of the

sequence and hence, are likely to need a customized validation strategy. This is especially relevant for phospho candidates since the context and localization probability of phosphorylation sites may vary widely from total protein abundance [24,25]. The biological significance of these proteins may also differ from that of the total protein abundance [26].

2.6. Confirmation Burden and Validation Sequence Index

Descriptor of confirmation burden represents the challenge faced while taking candidates from evidence listing to targeted validation process. The leakage indicator was defined as

$$Z_i = \begin{cases} 0, & \eta_i = 1, \\ 1, & \eta_i = 0.80. \end{cases} \tag{20}$$

The confirmation burden was then calculated as

$$\mathrm{CB}_i = 100\,[0.40(1-A_i) + 0.35(1-K_i) + 0.25Z_i]. \tag{21}$$

The mass-concordance factor gets the biggest weighting since the mass residual is important to the confidence of intact-form identification. The annotation uncertainty factor gets the second largest weighting since unknown or partially known modification patterns need structural validation. The leakage factor gets a small but definite weighting because control features at the lowest level influence candidate selection. The validation sequence index prioritizes both caution and validation effort:

$$\mathrm{VSI}_i = \mathrm{CAPS}_i^{(L)} \left(1 - \frac{\mathrm{CB}_i}{200}\right). \tag{22}$$

The value of 200 for the denominator makes the burden correction moderate rather than exclusionary. A candidate with a good CAPS score and a low burden stays early in the validation sequence, while a chemically interesting candidate with high burden is steered into a specific confirmation pathway.

2.7. Categories of Validation

The validation categories were determined based on the combined values of leakage-resistant CAPS, modification density, burden, and biological interpretability. The immediate candidates had both high conservative CAPS and low confirmation burden. Phosphorylation-specific validation was reserved for the candidates with a distinctive modification profile relying either on high density of phosphorylation sites or on specific evidence of PTMs. The annotation-resolved candidates needed additional information from their table entries about the exact composition and identity of their modifications. The exploratory fragments with small residue spans or poor proteochemistry were suitable for the future cleavage study but were not recommended for immediate assay development.

The categories did not reflect biological importance ranking. They reflected only the logic of the validation process. For instance, the well-known product of an inflammatory gene was considered the annotation-resolved candidate if there was no certainty about the identity of its proteoforms, whereas a less famous protein with specific evidence could be immediately validated. Such an approach was consistent with the requirement of the need for proteoform-specific claims for proteoform-specific evidence [19] especially if candidate selection started from top-down measurement of listed proteins [20].

3. Results and Discussion

3.1. Condition-Level form Pressure Revealed Proliferative form Composition

The condition block consisted of 201 intact-class proteoforms and 317 truncated proteoforms in total from the joint condition block record. The senescent secretome had 83 intact-class forms and 176 truncated forms, representing 259 total forms and truncated form pressure 0.67954. The quiescent secretome had 116 intact-class forms and 130 truncated forms, representing 246 total forms and truncated form pressure 0.52846. The proliferating secretome had 118 intact-class forms and 250 truncated forms, representing 368 total forms and truncated form pressure 0.67935. These numbers are shown in Table 2 and illustrated in Figure 1.

Table 2: Condition-level form pressure.

Condition	I_c	T_c	O_c	F_c	G_c	$\lvert F_S - F_c \rvert$
Senescent	83	176	259	0.67954	0.32046	0.00000
Quiescent	116	130	246	0.52846	0.47154	0.15108
Proliferating	118	250	368	0.67935	0.32065	0.00019
Combined	201	317	518	0.6120	0.3880	–

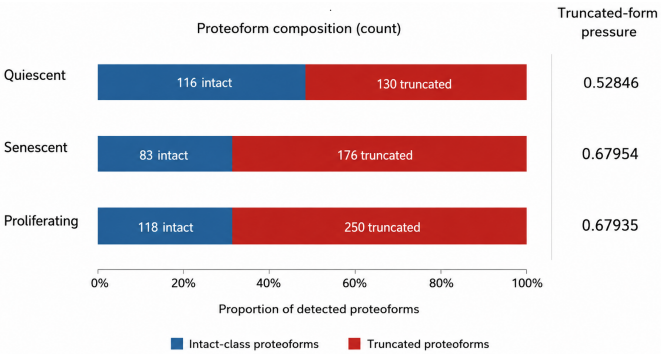

Figure 1: Proteoform composition by condition.

From the composition display in Figure 1, it is apparent that intact-class fraction is higher in quiescence, while senescence and proliferation both carry about the same level of truncated-form abundance. In the process, this graph also makes clear the control state for the late candidate: truncation is common in senescence but is not a senescence-specific phenomenon.

The essential point of Table 2 is not just that senescence is fragment-rich, but that proliferation is fragment-rich to the same extent. The senescence-quiescence distance was 0.15108, while the senescence-proliferation distance was 0.00019. The resulting ratio $R_{S,P}$ was 0.00125, while separation share Θ_S was 0.99875. Nearly all separation was, therefore, attributable to the comparison between senescence and quiescence. As a result, proliferation controls nearly overlapped with the senescent samples.

The intact-class fractions reinforce this point of view. Both senescence and proliferation were almost equally fragment-rich, with intact-class fractions of 0.32046 and 0.32065 respectively, while quiescence retained a higher intact-class fraction of 0.47154. In this scenario, the contrast is not between a fragment-rich senescence state and an otherwise intact non-senescent state. The three-state scenario sees quiescence being distinct, and proliferation closely following senescence on the form-pressure scale. As a consequence, the combined condition record, with 201 intact-class forms, 317 truncated forms and a form pressure of 0.6120, falls in between the quiescent and fragment-rich states and hence cannot serve as a sufficient control state for senescence specificity. Any validation sequence that ignores the above structure will favor fragments simply based on the fact that they appear in senescence but overlook the fact that truncation itself is a fragment-rich state characteristic of the condition block.

The distance figure itself affects how candidate classes should be interpreted. Since the senescence-proliferation distance of 0.00019 is about 800 times lower than the senescence-quiescence distance

of 0.15108, this does not disprove senescence-selective candidates. Rather, it shifts the burden of proof for different candidates. Long-span records with defined modification annotations can still be favored since they define identity beyond the fragment-rich background. Short fragments, on the other hand, require evidence that the span and mass of the fragment is uniquely associated with senescence and not just the fragment-rich background shared with proliferating cells. Therefore, the condition block serves as a control-state guardrail for all future candidate interpretation.

The distance plot in Figure 2 provides the key control-state result. While a senescent-versus-quiescent comparison reveals increased truncated form pressure, senescent-versus-proliferating comparison does not provide similar results since both distances are almost identical. The above pattern aligns with broader literature that shows that SASP interpretation depends on the choice of control state [27] and senescence context [6]. This explains why candidate-level chemistry is crucial: a fragment loses significance if the proliferating condition contains almost the same form-pressure background.

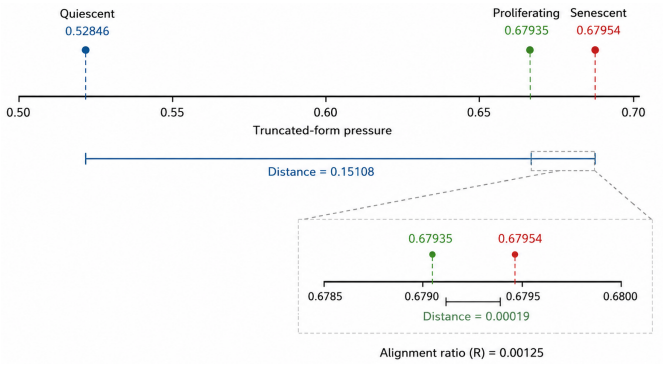

Figure 2: Dual-control form-pressure distance.

Consequently, Figures 1 and 2 reveal why candidate table needs to be read with a dual-control guardrail. Rather than reducing the importance of the candidate table, the above result changes the standard for candidate interpretation. Proteoform becomes more significant if its selectivity is confirmed through residue span, modification identity, mass residual, and leakage sensitivity and not merely through truncation. This consideration is especially relevant for proteins related to stress response, cytoskeleton turnover, secretion and extracellular modifications because such records can appear in multiple non-senescent stress states. Therefore, dual-control calculation provides a safety measure for one of the most common mistakes in secretome analysis: treating the presence in disease/stress-related samples as evidence of state specificity without considering the control state structure.

3.2. CAPS Separated Long-Span Candidates from Exploratory Fragments

Seven candidate records contained considerable variation in terms of residue span, modification annotation, mass residual, and leakage sensitivity. FTL had the largest residue span of 174 residues followed by UBE2V1 (146 residues), HMGA2 (108 residues) and DAP (101 residues). CCL2 spanned 76 residues while TPM3 and EEF1A1 contained 26 and 25 residues respectively. Residue span ranged from 0.980 Da (CCL2) to 1.239 Da (FTL). Annotations generated modification count of zero to five, with HMGA2 having the largest count.

The identity strip in Figure 3 depicts the candidates as records of the molecular sequence rather than simply as genes. FTL and UBE2V1 are the long-span records with known modifications, HMGA2 is marked by clustered phosphorylation, DAP and CCL2 have uncertain annotation, while TPM3 and EEF1A1 are represented by short non-modified fragments. This distinction clarifies why the validation order must keep the residue span and chemical state rather than grouping all the records into their parent genes.

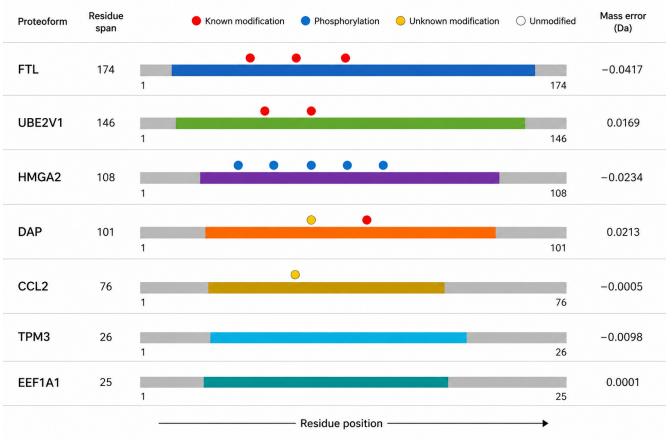

Figure 3: Candidate proteoform identity.

The CAPS descriptors in Table 3 separate immediate candidates from those requiring specific validation due to their special characteristics. FTL and UBE2V1 share long sequence span, known modifications and no leakage penalty. The HMGA2 is chemically significant with strict CAPS value of 82.39. The leakage-sensitive value is equal to 65.92 as low-level proliferating traces require cautious approach. It must not be interpreted as lack of biological significance but the requirement of a phospho-aware validation strategy for this candidate. The DAP and CCL2 belong to an intermediate group where the combination of span and biological plausibility is not sufficient in the case of unknown annotation. Finally, TPM3 and EEF1A1 remain in the low-priority category because of their insufficiently long spans.

Table 3: CAPS candidate descriptors.

Gene	Accession	Span residues	Mass error Da	P_i^s	K_i^s	CAPS$^{(0)}$	CAPS$^{(L)}$	Candidate status
FTL	P02792	174	1.239	3	3	77.61	77.61	Immediate
UBE2V1	Q13404	146	1.027	2	2	71.51	71.51	Immediate
HMGA2	P52926	108	1.002	5	5	82.39	65.92	Phosphorylation-specific
DAP	P51397	101	1.007	2	1	59.04	47.23	Annotation-resolved
CCL2	P13500	76	0.980	1	0	37.94	37.94	Annotation-resolved
TPM3	P06753	26	1.007	0	0	21.92	21.92	Exploratory
EEF1A1	P68104	25	1.007	0	0	21.55	21.55	Exploratory

This distinction between the candidates corresponds to the proteoform logic in top-down proteomics [28, 29] where whole protein or large proteoform measurements have a particular value in preserving molecular specificity [13] that cannot be achieved in peptide-centric and gene-name-centric analyses. FTL and UBE2V1 retain sufficient sequence and annotation information for early targeted analysis. The HMGA2 retains the PTM pattern but requires phospho-aware confirmation. Fragment records can be significant as well, but a fragment-heavy proliferating control environment does not support them as immediate markers of senescence.

The retained CAPS values demonstrate that the priority of the candidate is not determined by one value. Both FTL and UBE2V1 did not have any leakage penalty, and thus, their strict and leakage-sensitive CAPS values coincide: 77.61 and 71.51 respectively. The FTL has the largest span of 174 residues, 3 counted modification events and 3 known events with the mass residual of 1.239 Da. The UBE2V1 has 146-residue span, 2 counted and 2 known modification events and a small mass residual of 1.027 Da. As a result, the two candidates carry different advantages: FTL has the largest sequence span, while UBE2V1 has the lowest confirmation burden. Thus, their common immediate status is not arbitrary but a result of long sequence coverage, known chemical annotation and lack of the control-trace penalty.

The HMGA2 candidate demonstrates the opposite behavior: having

the largest strict CAPS value of 82.39 because it has 5 known modification events in 108-residue span, the low-level proliferating trace has reduced its leakage-sensitive CAPS value to 65.92. The DAP has lost its priority by the same reason, being reduced from the strict CAPS value of 59.04 to the leakage-sensitive value of 47.23. The CCL2 has not received the penalty for the leakage because it has no leakage penalty and the shorter 76-residue span and unknown modification annotation. The value of its CAPS is equal to 37.94. Finally, the short span of 26 residues and absence of counted modification evidence in the records of TPM3 and EEF1A1 have left them low priority. In other words, the ranking of the seven candidates is defined by their actual chemistry and not by the familiarity of the gene symbols.

The component fingerprint in Figure 4 shows why the candidates with the similar priorities are distinguished by the different proteoform properties. The FTL has the strongest support provided by the span and known modification identity. The UBE2V1 candidate has the balance between the span and mass concordance. The HMGA2 has the strong contribution of the modification burden but gets the moderation by leakage sensitivity. The DAP, CCL2, TPM3 and EEF1A1 lose their priorities by annotation uncertainty, shorter span or both of them. In other words, the matrix transforms the score into the interpretable proteoform record.

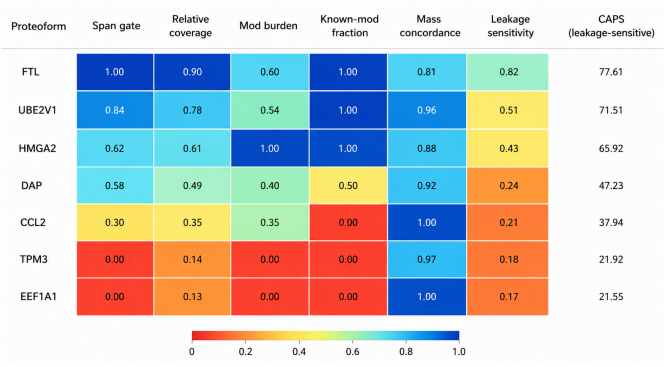

Figure 4: CAPS component fingerprint.

3.3. Modification Density Revealed a Chemically Distinct HMGA2 Signal

Residue-normalized modification density gave a different perspective on the candidate chemistry. FTL and UBE2V1 maintained top scores due to well-known modifications and long residue spans, while HMGA2 became obviously anomalous in terms of chemical concentration. HMGA2 has five known modifications among 108 residues, which makes up total and known modification density of 4.63 per 100 residues. FTL has three known modifications among 174 residues, which gives the density of 1.72 per 100 residues. UBE2V1 has two known modifications among 146 residues, making up 1.37 events per 100 residues. DAP has two total events among 101 residues but only one known event, making up total and known densities of 1.98 and 0.99 per 100 residues respectively. CCL2 has one total event among 76 residues but no known events according to the annotation rule, resulting in densities of 1.32 and 0 per 100 residues respectively. TPM3 and EEF1A1 have no modifications in counts.

The modification-density plot in Figure 5 separates the chemical concentration measure from the overall candidate priority. HMGA2 becomes the top high-density record, having 4.63 annotated events per 100 residues, while FTL and UBE2V1 represent a combination of low density and assay readiness. DAP and CCL2 represent the middle total-density region but lose interpretative power due to unclassified modification evidence. TPM3 and EEF1A1 have zero density. Such a result allows the practical recommendation that HMGA2 should be validated as phosphorylated proteoform rather than a total-HMGA2 abundance signal.

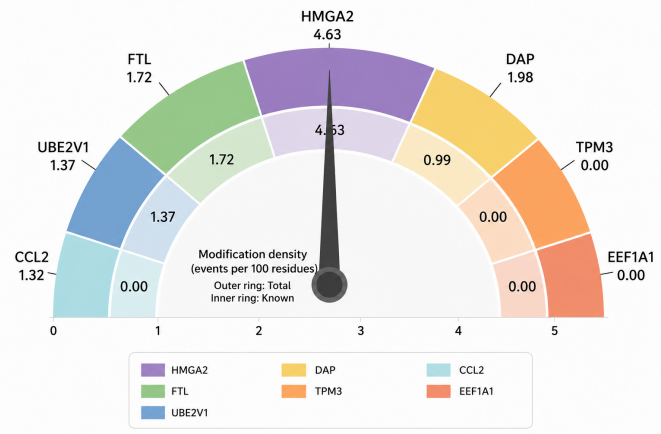

Figure 5: Modification-density distribution.

The high modification density of HMGA2 is biologically plausible considering the role of the protein in chromatin organization in senescence. HMGA proteins have been associated with chromatin structure and behavior of senescence-associated heterochromatin [30]. Modifications around nuclear localization or chromatin-binding regions may affect protein localization and interaction, which is generally shown for the case of nuclear import and protein trafficking regulation [31]. The comparison with the role of HMGB1 is also relevant since senescence-associated alarmins release may be related to protein retention in nucleus and controlled secretion [32]. These facts do not constitute a proof of any export pathway for HMGA2, but they create a rational background to choose HMGA2 for validation as a phosphorylated proteoform rather than total protein detection.

The modification density also explains why DAP and CCL2 should not be suggested based on gene-level reasoning. DAP has a moderate total density, however, only half of its modification evidence is classified as known modification according to the chosen rule. CCL2 is an obvious inflammatory chemokine, and chemokine biology is clearly relevant for SASP. However, the candidate record has an unknown modification and shorter residue span. Thus, the question to address for CCL2 is not if CCL2 is a known inflammatory mediator, but whether the detected CCL2 proteoform has confirmed identity, consistent mass assignment and senescence selectivity. This distinction saves the analysis from confirmation bias towards recognizable SASP names.

3.4. The Confirmation-Burden Computation Turned Prioritization into Validation

The confirmation-burden computation added an aspect of realism to the ranking process. UBE2V1 had the smallest burden of 27.39 since it is known to have annotation, good mass correlation, and lack of leakage penalty. The burden of FTL was 33.04 and this was due to large mass residual but balanced with good annotation and lack of control-trace penalty. HMGA2 had a burden of 51.72 since it had a good chemical signal but the presence of control-trace penalty reduced it. DAP had the largest burden of 69.35 since it had leakage sensitivity as well as partial annotation uncertainty. The burden of CCL2 was 61.13 since there was uncertainty about the modification of the protein under the counting rule. TPM3 and EEF1A1 each had a burden of 44.35 because their unmodified status was treated neutrally but their mass-concordance weakness remained.

The readiness order in Figure 6 separates the seven records into four assay classes. FTL and UBE2V1 belong to the immediate class, since both involve highly leakage-sensitive CAPS with acceptable confir-

mation burdens. HMGA2 belongs to a phosphorylation-specific class, whose value is based on the modified proteoform, rather than the overall protein abundance. DAP and CCL2 belong to an annotation-resolved class, while TPM3 and EEF1A1 are short-fragment candidates for later boundary testing.

Immediate validation (long-span, known modification)	CAPS (leakage-sensitive)	Confirmation burden
FTL	77.61	33.04
UBE2V1	71.51	27.39
Phosphorylation-specific confirmation	**CAPS (leakage-sensitive)**	**Confirmation burden**
HMGA2	65.92	51.72
Annotation-resolved confirmation	**CAPS (leakage-sensitive)**	**Confirmation burden**
DAP	47.23	69.35
CCL2	37.94	61.13
Exploratory fragments (short, unmodified)	**CAPS (leakage-sensitive)**	**Confirmation burden**
TPM3	21.92	44.35
EEF1A1	21.55	44.35

Figure 6: Candidate readiness order.

The validation descriptors in Table 4 should be considered a validation readiness sequence, not a sequence of biological relevance. FTL and UBE2V1 are prioritized at the top, because they are the most validation-ready candidates in the listed evidence structure. HMGA2 is ranked at the third position not because of its lower biological interest, but because it requires a special assay which can resolve the phosphoforms and assess low-level traces. DAP and CCL2 are ranked after because annotation uncertainty should be solved before their use to conclude about the mechanism. TPM3 and EEF1A1 are retained, but due to their short span and poor chemistry, cannot be used as primary validation targets. This distinction reflects the present senescence-marker guideline: a molecular readout should not be promoted as a state marker until the knowledge about its context, detection basis, and specificity limitations are clarified [6, 9].

Table 4: Validation descriptors and candidate sequence.

Gene	MD per 100 residues	KMD per 100 residues	CB	VSI	Order	Validation interpretation
FTL	1.72	1.72	33.04	64.79	1	Immediate intact-form validation with modification-aware readout
UBE2V1	1.37	1.37	27.39	61.72	2	Immediate long-span proteoform assay with proteostasis-focused interpretation
HMGA2	4.63	4.63	51.72	48.87	3	Phosphorylation-specific follow-up after control-trace evaluation
DAP	1.98	0.99	69.35	30.85	4	Annotation-resolved confirmation before mechanistic ranking
CCL2	1.32	0.00	61.13	26.34	5	Chemokine proteoform identity check before inflammatory interpretation
TPM3	0.00	0.00	44.35	17.06	6	Exploratory fragment retained for later cleavage-focused assays
EEF1A1	0.00	0.00	44.35	16.77	7	Exploratory fragment retained for later stress-processing assays

The burden decomposition in Figure 7 explains why the follow-up difficulty of candidate does not scale with CAPS only. UBE2V1 and FTL have lower confirmation burden because of known modifications and low level of control traces. HMGA2 has larger burden, since the phosphorylation-rich signal needs to be checked against proliferating traces. DAP and CCL2 need the largest amount of identity work because annotation uncertainty is the direct contributor to the confirmation burden. The confirmation burden values for TPM3 and EEF1A1 are moderate, but they stay at low priority because of short spans and weak chemistry of their proteoforms.

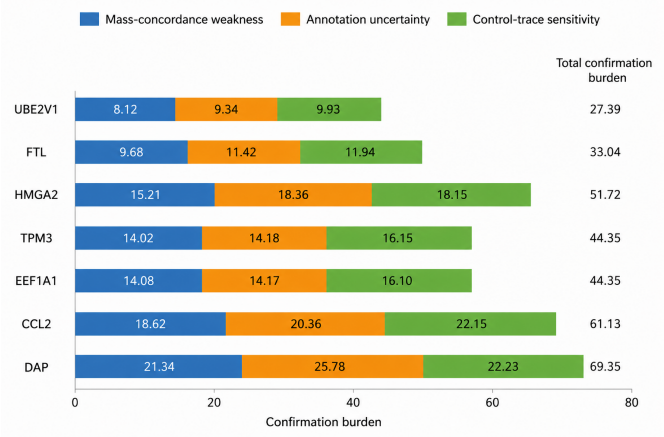

Figure 7: Confirmation-burden components.

The sequence plate in Figure 8 shows the final order as candidate-specific assignments. FTL and UBE2V1 take leading positions because of their long spans and known modifications. HMGA2 is kept in the prominent position because of its phosphorylation density. DAP and CCL2 are kept in the plate after resolving annotation uncertainty, while TPM3 and EEF1A1 are retained for fragment-boundary testing. This plate makes it impossible to interpret the validation sequence as a protein list, since each row describes specific molecular reasons for keeping the particular record.

This result fits well with practical requirements of targeted proteomics. Candidate selected for follow-up needs to be transformed into assay. Parallel reaction monitoring and selected reaction monitoring can quantitatively measure proteins or peptides in a reproducible way [33, 34]. Data-independent acquisition and targeted extraction can provide alternative solutions [35, 36], but proteoform-specific claims require a very careful selection of transitions, precursor forms, fragment ions, modifications-specific evidence, and proper controls. Skyline and other similar tools allow making targeted proteomics easier, but still depend on a molecular target [37]. In this case, the validation sequence provides the necessary triaging before building an assay.

Rank	Proteoform candidate	Validation sequence index (VSI)	Validation class	Proteoform-specific reason
1	FTL	64.79	Immediate	Long span, known modifications
2	UBE2V1	61.72	Immediate	Long span, known modifications
3	HMGA2	48.87	Phosphorylation-specific	High phosphorylation density
4	DAP	30.85	Annotation-resolved	Unknown modification annotation
5	CCL2	26.34	Annotation-resolved	Unknown modification annotation
6	TPM3	17.06	Exploratory fragment	Short span, unmodified fragment
7	EEF1A1	16.77	Exploratory fragment	Short span, unmodified fragment

Figure 8: Validation sequence index.

3.5. FTL and UBE2V1 Warrant Immediate Long-Span Validation

FTL had the highest rank in the validation sequence, with a leakage-adjusted CAPS of 77.61, confirmation burden of 33.04, and validation sequence index of 64.79. It has the longest span of 174 residues and complete modification annotation. Its biological interpretation should be careful: FTL is a protein involved in iron metabolism, oxidative stress, and inflammatory response that all play a role in SASP biology. But while the calculation validates the detected proteoform, it does not validate a general statement about total abundance of FTL being a marker of SASP. An appropriate validation assay should aim to preserve the intact form or modification annotation whenever possible.

UBE2V1 ranked second with a leakage-adjusted CAPS of 71.51, the lowest confirmation burden of 27.39, and validation sequence index of 61.72. Residue span of 146 and known modification annotation make UBE2V1 a strong candidate for immediate validation. The relevance to proteostasis biology is plausible due to ubiquitination and NEDD8-stress-response mechanisms being often affected during aging [38]. While CAPS result does not show any specifics of a pathway of ubiquitination in the secretome, it confirms that the UBE2V1 proteoform has enough coherence regarding span, modification annotation, and mass agreement to warrant targeted confirmation.

Both FTL and UBE2V1 belong to the same validation class, since they depend less on PTM localization, and have no unknown annotation unlike DAP and CCL2. They are therefore good candidates to determine whether the same proteoform records can be validated in a targeted manner. Failure of validation of either candidate would reduce confidence in lower-ranked candidates; success of validation of both would allow rational transition to more specialized PTM and annotation-validation experiments.

3.6. HMGA2 Demands Phosphorylation-Specific Confirmation

HMGA2 has the most chemical diversity among candidates in the analysis. Strict CAPS of 82.39 made it the candidate with the highest CAPS in the analysis. Moreover, it has the highest modification density of 4.63 events per 100 residues, being more than twice higher than in FTL and UBE2V1. The conservative leakage adjustment brought its CAPS to 65.92, and confirmation burden was 51.72. This places HMGA2 below FTL and UBE2V1 in the validation sequence, but above all annotation-resolved and exploratory candidates.

The key point here is that HMGA2 is not a target for measuring total protein abundance. Its candidate signal is a phosphorylated proteoform signal. If the validation procedure involves an assay that cannot distinguish phospho-HMGA2 from the total protein, it will not confirm the original observation. An appropriate approach here would be an intact form or targeted MS, as well as phospho-specific enrichment where applicable, and fragment-ion confirmation of the phosphorylation region. This makes the candidate highly valuable, but increases assay burden considerably compared to FTL and UBE2V1.

The conclusion corresponds to the existing body of knowledge regarding senescence associated chromatin regulation. HMGA-family proteins are involved in chromatin organization, and HMGA2-related modifications have been linked to the senescence associated nuclear state [39]. Secretome context also allows assuming that altered localization and release can be involved as the part of SASP. Similar questions arise when considering HMGB1, an alarmin whose senescence-associated release was investigated in terms of nuclear regulation and inflammatory signaling [40]. These examples support the interest in the target, but do not prove the localization or release mechanism. The conclusion is that phosphorylation-specific validation experiment is warranted.

3.7. DAP and CCL2 need Annotation-Resolved Interpretation

DAP and CCL2 exemplify cases where biological knowledge alone is not enough for correct candidate selection. DAP had a leakage-sensitive CAPS value of 47.23 and confirmation burden of 69.35. Residue span was adequate for both proteins. However, only one out of two counted modification events could be considered known. High confirmation burden means that DAP should not be used as a potential anchoring point at once and needs an annotation resolution with the help of targeted fragmentation or another orthogonal technique.

CCL2 had a somewhat lower leakage-sensitive CAPS value of 37.94 and a confirmation burden of 61.13. From the gene level perspective, CCL2 is a promising candidate since chemokines play important role in inflammatory SASP biology. However, at proteoform level, CCL2 record is much less ready for a use in a mechanistic study. The 76-residue span is shorter than the major long-span candidates, and the modification annotation is unknown in this classification. Thus, a CCL2 follow-up assay must start with the proteoform identification and confirmation of the mass shift. Only then the record can be used as evidence of a certain inflammatory SASP proteoform.

The findings for DAP and CCL2 show one of the important benefits of a control-aware proteoform sequence. Conventional discussion of the results would pay more attention to CCL2 because it is a well-known inflammatory mediator. In the control-aware validation sequence, however, the molecular record is appropriately constrained by molecular evidence. That does not mean that CCL2 lacks biological significance. It just prevents an overstatement. A proteoform-level manuscript should not let the popularity of a gene symbol affect the candidate order.

3.8. TPM3 and EEF1A1 are Exploratory Fragment Records

TPM3 and EEF1A1 are ranked sixth and seventh in the validation sequence. TPM3 has a span of 26 residues, no counted modifications, leakage-sensitive CAPS value of 21.92, and validation sequence index of 17.06. EEF1A1 has a span of 25 residues, no counted modifications, leakage-sensitive CAPS value of 21.55, and validation sequence index of 16.77. Their confirmation burdens are not among the largest ones in the panel due to neutral treatment of unmodified records in accordance with the known modification fraction rule. The low indices of these candidates are explained by the relatively short span and lack of proteochemical information.

The two records should not be discarded. Fragment records may report biologically significant cleavage, extracellular processing, stress-induced proteolysis, or sample state difference. However, the condition-level analysis makes their interpretation quite problematic. Proliferating secretomes were practically the same as the senescent ones in terms of truncated form pressure. Thus, fragments need a particularly strong evidence before being considered as a proof of the senescence selectivity. TPM3 and EEF1A1 should be retained for later analyses that are focused on the origin of the fragment, cleavage boundaries, and the candidate behavior in control conditions. They should not be ranked above long-span proteoforms with clear chemical annotation.

This ranking reflects a practical consideration that is useful in top-down secretome studies. Fragment records are valuable in the case of consistent cleavage patterns, condition specificity, and mechanistic context. In the absence of this context, they are worse candidates for biomarkers than long-span, chemically coherent proteoforms. That is why the validation sequence is conservative. It protects the downstream experiments from spending assay development resources on fragments that may represent a general proteolytic or extracellular processing pressure rather than senescence-specific secretion.

3.9. Implications for SASP Biomarker Development

The main implication of this analysis is that the proteoform-level SASP biomarkers require a two-layer selection logic. The first layer asks whether the condition context is suitable for the senescence-specific interpretation. The second layer asks whether the molecular record is specific enough to be considered a good candidate for the targeted validation. The two layers are independent. A candidate may be listed in a senescence-selective table, but it may be weak due to the ambiguous condition context or chemically unresolved proteoform identity. On the contrary, a candidate may have good validation value despite having an unfamiliar gene name.

This logic fits with the development of aging biomarkers and senescence interventions. Senescent cells are increasingly considered as contributing factors to age-related pathology and therapeutic targets [41,42]. The secretome measurements are interesting due to the accessibility of extracellular molecules. But the accessibility is not equal to the specificity. SASP measurements can be confused by the existence of several proteoforms or missed by total abundance assays. Top-down measurements can help with this issue, but the candidates should be filtered out before performing expensive validation assays.

The validation sequence also allows determining the optimal assay technology. FTL and UBE2V1 are candidates that can be investigated with intact-form aware or modification-aware targeted method. HMGA2 requires phosphorylation-specific confirmation. DAP and CCL2 need annotation-resolved experiments before making a claim about the mechanism of their secretion. TPM3 and EEF1A1 require fragment-focused follow-up if they are still interesting. This way, the candidates are mapped to the specific validation problem instead of being analyzed with the same protocol.

3.10. Assay Design Consequences of the Validation Sequence

The validation sequence has implications for experimental design. For both FTL and UBE2V1, the key point of the next experiment is consistent detection of the same span proteoform records in senescence and control secretomes. Since both of them already have annotation of the modification sites and no leakage penalty, the question is whether it is possible to recover the listed molecular forms with acceptable consistency under targeted acquisition mode. In case of the intact protein or middle-down approach the best choice, while a peptide-based design will require special attention to selecting peptides that don't destroy the molecular form responsible for the record. In case of peptide-based assay the record should be considered as supporting abundance evidence but not as confirmation of the molecular form.

For HMGA2 the design issue is quite another. It is not HMGA2, but its dense phosphorylation that is supposed to be validated in a certain span proteoform record. Therefore, the right approach will be a phospho-sensitive workflow rather than a total-HMGA2 quantification. In addition, the control trace sensitivity makes proliferating samples inappropriate to use as a secondary comparator since the form pressure analysis showed near-total agreement between senescent and proliferating environments for truncated forms. So the right design will be including proliferating samples in the main group with equal priority.

Consequently, the order of the assays is not ambiguous regarding the experimental design since it does not include the ambiguous narrative category. Firstly, FTL and UBE2V1 must be tested for the recovery of the same span proteoform records in senescent, quiescent and proliferating secretomes. Secondly, HMGA2 must be validated with a phospho-sensitive design. Thirdly, DAP and CCL2 must have their identity clarified before the pathway interpretation since they lack complete annotation of modifications. Lastly, TPM3 and EEF1A1 are the boundary fragment candidates, so they require fragmentation confirmation before biomarker interpretation. The given sequence is implied directly by spans, number of modifications, mass residuals, leakage, confirmation burden and validation index.

The validation sequence implies the following assay design in Figure 9. FTL and UBE2V1 need the confirmation of their intact mass and modification state. HMGA2 needs confirmation of site-specific phosphorylation. DAP and CCL2 need the clarification of unknown or partly known mass shifts. Lastly, TPM3 and EEF1A1 need confirmation of the reproducible cleavage boundaries. Thus, the practical value of the validation sequence is not only ranking, but assigning the specific confirmation need to each proteoform category.

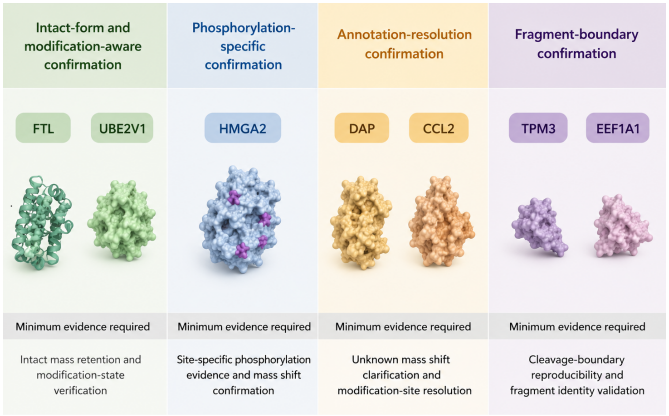

Figure 9: Assay-specific confirmation needs.

The order itself helps to avoid misinterpretation of the well-known biology. CCL2 is a known inflammatory chemokine, but the proteoform record is shorter than those of FTL, UBE2V1, HMGA2 and DAP and has no known modifications in this classification. HMGA2 is biologically connected to chromatin and senescence-related nuclear states, but the priority of the record depends on phosphorylation density, and not total HMGA2 abundance. The proteoforms of FTL and UBE2V1 may not be related immediately to a canonical SASP cytokine story, but have the strongest validation features. Thus, the interpretation of the data should follow the proteoform evidence: long span, chemically annotated proteoforms first, dense phosphorylation with control trace sensitivity second, uncertain proteoforms third and fragments last.

DAP and CCL2 require an additional step. The primary end point for these two candidates should be identity resolution, and not immediate pathway interpretation. Additional fragmentation, alternative search settings, targeted inspection of the unknown mass shift, or orthogonal enrichment could help to clarify whether the table annotation corresponds to a real biological proteoform. Then, after this step the interpretation of DAP in relation to cell stress biology and of CCL2 in relation to inflammatory SASP signaling could be appropriate. The given order is especially important for CCL2 due to its gene-level biological familiarity. The validation sequence avoids the potential bias by requiring the identity of the proteoform before any biological interpretation.

TPM3 and EEF1A1 make the exploratory edge of the candidate set. Their value is related to the questions about cleavage, extracellular processing and stress-related fragmentation, not to immediate biomarker development. The key confirmation criteria here are reproducible fragment boundaries, consistent fragment abundance in senescence induction and separation from proliferating controls in matched culture and collection conditions. Until all these tests are completed, these two records should be put after the long span and chemically annotated candidates. Thus, the candidate-specific assay assignment avoids wasted effort and helps to preserve molecular specificity of the top-down SASP proteomics.

3.11. Boundary of Interpretation for the Validation Order

The computation is deterministic and relies solely on the condition counts and candidate fields. The computation does not compute statistical significance, variance of the replicates, effect size confidence intervals, localization probability at the site level, or reproducibility of the chromatography. The mass residual is a practical measure and not an error model. The fraction of known modifications is a confidence descriptor and not a biochemical one. The leakage adjustment is a sensitivity factor and not an abundance measure.

These boundaries delimit the correct use of the validation order. The seven SASP candidates cannot be considered fully validated. What can be claimed is that the counts and fields make a reasonable validation sequence that is more informative than a gene rank list. The sequence takes care of condition, chemistry, mass agreement, annotation interpretability, and validation burden. The sequence reveals the core dual control issue: senescence and proliferation were very close in truncated-form pressure, and fragment rich observations must be treated carefully.

The boundaries are candidate specific. FTL and UBE2V1 need intact-form confirmation. HMGA2 needs phosphorylation-specific confirmation. DAP and CCL2 need annotation resolution. TPM3 and EEF1A1 need fragment origin testing. Quantification aware of the replicates, raw spectra assessment, confirmation by intact or middle-down experiments, and orthogonal confirmation would test the assignments, but the order derives from the listed spans, masses, modification annotations, control traces, and confirmation burden.

4. Conclusion

The research question was whether the top-down proteomics records of the senescent, quiescent, and proliferating human fibroblasts secretomes would support a defensible proteoform validation order while maintaining the CAPS calculation. The answer is yes, but condition and proteoform chemistry must be interpreted together. Senescence was not a fragment rich state compared to all controls. The senescent and proliferating forms had almost identical truncated-form pressures of 0.67954 and 0.67935 respectively. The quiescent forms had a lower value of 0.52846. The ratio between the senescence-proliferation pressures of 0.00125 revealed that truncation pressure distinguished senescence from quiescence but not from proliferation. Fragment abundance cannot be used alone as a signal of senescence selectivity.

The candidate-level analysis answered the validation aspect of the question. FTL and UBE2V1 are the first targets because they combine the largest spans, known modification annotations, highest leakage-sensitive CAPS, and acceptable confirmation burden. HMGA2 is the most chemically distinct candidate because it has 4.63 mass shift events per 100 residues but this number points to the need of phosphorylation specific validation rather than HMGA2 measurement as a whole. DAP and CCL2 need annotation resolution before biological interpretation. TPM3 and EEF1A1 need fragment origin testing before confirmation of their cleavage boundaries and control-state selectivity. The order becomes clear and candidate-specific: FTL and UBE2V1 first, HMGA2 through phosphorylation-aware confirmation, DAP and CCL2 after annotation resolution, and TPM3 and EEF1A1 after fragment-boundary testing.

The analysis provided the interpretation of a proteoform score in the difficult case of three-state comparison. By bringing together condition form pressure, residue span, modification identity, mass agreement, leakage sensitivity, and confirmation burden, the manuscript avoids two common mistakes in SASP proteomics: fragment-rich output is not automatically senescence-specific and parent protein names do not substitute for molecular evidence. The conclusion is specific to these IMR90 secretome records: a candidate list of SASP proteoforms becomes experimentally useful only when it turns into candidate-specific validation questions.

References

[1] Muñoz-Espín, D., & Serrano, M. (2014). Cellular senescence: from physiology to pathology. Nature reviews Molecular cell biology, 15(7), 482-496.

[2] Hernandez-Segura, A., Nehme, J., & Demaria, M. (2018). Hallmarks of cellular senescence. Trends in cell biology, 28(6), 436-453.

[3] Gorgoulis, V., Adams, P. D., Alimonti, A., Bennett, D. C., Bischof, O., Bishop, C., ... & Demaria, M. (2019). Cellular senescence: defining a path forward. Cell, 179(4), 813-827.

[4] Coppé, J. P., Patil, C. K., Rodier, F., Sun, Y. U., Muñoz, D. P., Goldstein, J., ... & Campisi, J. (2008). Senescence-associated secretory phenotypes reveal cell-nonautonomous functions of oncogenic RAS and the p53 tumor suppressor. PLoS biology, 6(12), e301.

[5] Malaquin, N., Martinez, A., & Rodier, F. (2016). Keeping the senescence secretome under control: molecular reins on the senescence-associated secretory phenotype. Experimental gerontology, 82, 39-49.

[6] Wang, B., Han, J., Elisseeff, J. H., & Demaria, M. (2024). The senescence-associated secretory phenotype and its physiological and pathological implications. Nature Reviews Molecular Cell Biology, 25(12), 958-978.

[7] Wiley, C. D., Velarde, M. C., Lecot, P., Liu, S. U., Sarnoski, E. A., Freund, A., ... & Campisi, J. (2016). Mitochondrial dysfunction induces senescence with a distinct secretory phenotype. Cell metabolism, 23(2), 303-314.

[8] Herranz, N., & Gil, J. (2018). Mechanisms and functions of cellular senescence. The Journal of clinical investigation, 128(4), 1238-1246.

[9] Ogrodnik, M., Acosta, J. C., Adams, P. D., di Fagagna, F. D. A., Baker, D. J., Bishop, C. L., ... & Demaria, M. (2024). Guidelines for minimal information on cellular senescence experimentation in vivo. Cell, 187(16), 4150-4175.

[10] Basisty, N., Kale, A., Jeon, O. H., Kuehnemann, C., Payne, T., Rao, C., ... & Schilling, B. (2020). A proteomic atlas of senescence-associated secretomes for aging biomarker development. PLoS biology, 18(1), e3000599.

[11] Samiminemati, A., Aprile, D., Siniscalco, D., & Di Bernardo, G. (2024). Methods to investigate the secretome of senescent cells. Methods and Protocols, 7(4), 52.

[12] Smith, L. M., & Kelleher, N. L. (2013). Proteoform: a single term describing protein complexity. Nature methods, 10(3), 186-187.

[13] Smith, L. M., & Kelleher, N. L. (2018). Proteoforms as the next proteomics currency. Science, 359(6380), 1106-1107.

[14] LeDuc, R. D., Deutsch, E. W., Binz, P. A., Fellers, R. T., Cesnik, A. J., Klein, J. A., ... & Vizcaíno, J. A. (2022). Proteomics standards initiative's ProForma 2.0: unifying the encoding of proteoforms and peptidoforms. Journal of proteome research, 21(4), 1189-1195.

[15] Tran, J. C., Zamdborg, L., Ahlf, D. R., Lee, J. E., Catherman, A. D., Durbin, K. R., ... & Kelleher, N. L. (2011). Mapping intact protein isoforms in discovery mode using top-down proteomics. Nature, 480(7376), 254-258.

[16] Catherman, A. D., Durbin, K. R., Ahlf, D. R., Early, B. P., Fellers, R. T., Tran, J. C., ... & Kelleher, N. L. (2013). Large-scale top-down proteomics of the human proteome: membrane proteins, mitochondria, and senescence. Molecular & Cellular Proteomics, 12(12), 3465-3473.

[17] Fornelli, L., Durbin, K. R., Fellers, R. T., Early, B. P., Greer, J. B., LeDuc, R. D., ... & Kelleher, N. L. (2017). Advancing top-down analysis of the human proteome using a benchtop quadrupole-orbitrap mass spectrometer. Journal of proteome research, 16(2), 609-618.

[18] Chen, B., Brown, K. A., Lin, Z., & Ge, Y. (2017). Top-down proteomics: ready for prime time?. Analytical chemistry, 90(1), 110-127.

[19] Roberts, D. S., Loo, J. A., Tsybin, Y. O., Liu, X., Wu, S., Chamot-Rooke, J., ... & Ge, Y. (2024). Top-down proteomics. Nature Reviews Methods Primers, 4(1), 38.

[20] Po, A., & Eyers, C. E. (2023). Top-down proteomics and the challenges of true proteoform characterization. Journal of proteome research, 22(12), 3663-3675.

[21] Boroumand, M., Dey, A., Cupp-Sutton, K., Pierce, T., Tsitsipatis, D., Herman, A. B., ... & Basisty, N. (2025). Characterization of the Intact Proteomic Profile of Senescent-Associated Secretory Phenotype by Top-Down Mass Spectrometry. Analytical chemistry, 97(47), 25967-25978.

[22] Perez-Riverol, Y., Bai, J., Bandla, C., García-Seisdedos, D., Hewapathirana, S., Kamatchinathan, S., ... & Vizcaíno, J. A. (2022). The PRIDE database resources in 2022: a hub for mass spectrometry-based proteomics evidences. Nucleic acids research, 50(D1), D543-D552.

[23] Brown, K. A., Melby, J. A., Roberts, D. S., & Ge, Y. (2020). Top-down proteomics: challenges, innovations, and applications in basic and clinical research. Expert review of proteomics, 17(10), 719-733.

[24] Olsen, J. V., & Mann, M. (2013). Status of large-scale analysis of post-translational modifications by mass spectrometry. Molecular & cellular proteomics, 12(12), 3444-3452.

[25] Riley, N. M., & Coon, J. J. (2016). Phosphoproteomics in the age of rapid and deep proteome profiling. Analytical chemistry, 88(1), 74-94.

[26] Doll, S., & Burlingame, A. L. (2015). Mass spectrometry-based detection and assignment of protein posttranslational modifications. ACS chemical biology, 10(1), 63-71.

[27] Hernandez-Segura, A., de Jong, T. V., Melov, S., Guryev, V., Campisi, J., & Demaria, M. (2017). Unmasking transcriptional heterogeneity in senescent cells. Current Biology, 27(17), 2652-2660.
[28] Aebersold, R., Agar, J. N., Amster, I. J., Baker, M. S., Bertozzi, C. R., Boja, E. S., ... & Zhang, B. (2018). How many human proteoforms are there?. Nature chemical biology, 14(3), 206-214.
[29] Toby, T. K., Fornelli, L., & Kelleher, N. L. (2016). Progress in top-down proteomics and the analysis of proteoforms. Annual review of analytical chemistry, 9(1), 499-519.
[30] Kuwayama, N., Kujirai, T., Kishi, Y., Hirano, R., Echigoya, K., Fang, L., ... & Gotoh, Y. (2023). HMGA2 directly mediates chromatin condensation in association with neuronal fate regulation. Nature Communications, 14(1), 6420.
[31] Harreman, M. T.; Kline, T. M.; Milford, H. G.; Harben, M. B.; Hodel, A. E.; Corbett, A. H. Regulation of nuclear import by phosphorylation adjacent to nuclear localization signals. *Journal of Biological Chemistry* **2004**, *279*, 20613–20621. Kuwayama, N., Kujirai, T., Kishi, Y., Hirano, R., Echigoya, K., Fang, L., ... & Gotoh, Y. (2023). HMGA2 directly mediates chromatin condensation in association with neuronal fate regulation. Nature Communications, 14(1), 6420.
[32] Davalos, A. R., Kawahara, M., Malhotra, G. K., Schaum, N., Huang, J., Ved, U., ... & Campisi, J. (2013). p53-dependent release of Alarmin HMGB1 is a central mediator of senescent phenotypes. Journal of Cell Biology, 201(4), 613-629.
[33] Peterson, A. C., Russell, J. D., Bailey, D. J., Westphall, M. S., & Coon, J. J. (2012). Parallel reaction monitoring for high resolution and high mass accuracy quantitative, targeted proteomics. Molecular & cellular proteomics, 11(11), 1475-1488.
[34] Gillet, L. C., Navarro, P., Tate, S., Röst, H., Selevsek, N., Reiter, L., ... & Aebersold, R. (2012). Targeted data extraction of the MS/MS spectra generated by data-independent acquisition: a new concept for consistent and accurate proteome analysis. Molecular & Cellular Proteomics, 11(6).
[35] Röst, H. L., Rosenberger, G., Navarro, P., Gillet, L., Miladinović, S. M., Schubert, O. T., ... & Aebersold, R. (2014). OpenSWATH enables automated, targeted analysis of data-independent acquisition MS data. Nature biotechnology, 32(3), 219-223.
[36] Ludwig, C., Gillet, L., Rosenberger, G., Amon, S., Collins, B. C., & Aebersold, R. (2018). Data-independent acquisition-based SWATH-MS for quantitative proteomics: a tutorial. Molecular systems biology, 14(8), MSB178126.
[37] MacLean, B., Tomazela, D. M., Shulman, N., Chambers, M., Finney, G. L., Frewen, B., ... & MacCoss, M. J. (2010). Skyline: an open source document editor for creating and analyzing targeted proteomics experiments. Bioinformatics, 26(7), 966-968.
[38] Maghames, C. M., Lobato-Gil, S., Perrin, A., Trauchessec, H., Rodriguez, M. S., Urbach, S., ... & Xirodimas, D. P. (2018). NEDDylation promotes nuclear protein aggregation and protects the Ubiquitin Proteasome System upon proteotoxic stress. Nature communications, 9(1), 4376.
[39] Narita, M., Narita, M., Krizhanovsky, V., Nuñez, S., Chicas, A., Hearn, S. A., ... & Lowe, S. W. (2006). A novel role for high-mobility group a proteins in cellular senescence and heterochromatin formation. Cell, 126(3), 503-514.
[40] Chen, R., Kang, R., & Tang, D. (2022). The mechanism of HMGB1 secretion and release. Experimental & molecular medicine, 54(2), 91-102.
[41] Schafer, M. J., White, T. A., Iijima, K., Haak, A. J., Ligresti, G., Atkinson, E. J., ... & LeBrasseur, N. K. (2017). Cellular senescence mediates fibrotic pulmonary disease. Nature communications, 8(1), 14532.
[42] Childs, B. G., Durik, M., Baker, D. J., & Van Deursen, J. M. (2015). Cellular senescence in aging and age-related disease: from mechanisms to therapy. Nature medicine, 21(12), 1424-1435.